ELSEVIER

Inorganica Chimica Acta 337 (2002) 287–298

Inorganica Chimica Acta

www.elsevier.com/locate/ica

X-ray crystallographic and NMR spectroscopical characterization of intermediates in the Pd-catalyzed allylic substitution reaction with 4-substituted phosphinooxazolines. Correlation between intermediate structure and product configuration

Margareta Zehnder [a], Silvia Schaffner [a], Markus Neuburger [a], Dietmar A. Plattner [b,*]

[a] *Institut für Anorganische Chemie der Universität Basel, Spitalstrasse 51, CH-4056 Basel, Switzerland*

[b] *Laboratorium für Organische Chemie der Eidgenössischen Technischen Hochschule Zürich, ETH-Hönggerberg, HCI, CH-8093 Zürich, Switzerland*

Received 11 March 2002; accepted 25 April 2002

Dedicated to Professor Karl Wieghardt on the occasion of his 60th birthday in recognition of his many outstanding contributions to coordination chemistry.

Abstract

The novel P,N-ligand 2-[2-(diphenylphosphino)phenyl]-4,5-dihydro-4-methyl-4-phenyloxazole (**2a**) has been synthesized. The corresponding [Pd^{II}(η^3-diphenylallyl) (**2a**)]PF_6 (**3a**) and [Pd^{II}(η^3-1,3-dimethylallyl) (**2a**)]PF_6 (**4a**) complexes have been studied by X-ray analysis and NMR spectroscopy. **3a** exists as *exo–syn–syn* isomer in the solid state. In solution, the same isomer predominates. The X-ray structure of **4a** reveals that the oxazoline ligand is coordinated in a pseudo-enantiomeric conformation compared with **3a**. A *syn–anti* arrangement of the allyl substituents is favored in the solid state. NMR spectroscopical investigations suggest a formation of six isomers in solution due to *endo–exo* orientation of the allyl moiety and *syn–anti* isomerization of the methyl substituents. NMR data of [Pd^0(η^2-dimethylfumarate)(phosphinooxazoline)] complexes give evidence that two isomers exist in solution. The isomeric ratio is strongly dependent on the steric bulk of the oxazoline substituents. The solid state structures of [Pd^0(η^2-dmfu) (**2c**)] and [Pd^0(η^2-dmfu) (**1a**)] confirmed the structures of the main isomer found in solution. The asymmetric allylic substitution reaction of 1,3-diphenylallyl acetate with dimethyl malonate catalyzed by **3a** proceeds with a selectivity of 97% ee. The ee induced by **2a** in catalytic allylic substitution of 1-methylbutenyl acetate is moderate (18%). A comparison of the intermediate **4a** and **5a** as model of the actual olefinic intermediate suggests that the poor enantioselectivity achieved with ligand **2a** is due to the preferred formation of *anti*-isomers of the allylic intermediate **4a** and the conformational instability of the complex.

Keywords: Pd(η^2-alkene) compounds; Pd(η^3-allyl) compounds; Phosphinooxazoline ligands; Enantioselective catalysis; Allylic substitution reaction

1. Introduction

Chiral 4-substituted 2-[2-(diphenylphosphino)phenyl]-4,5-dihydrooxazole ligands (phosphinooxazolines) (**1**) have been applied in a number of asymmetric transition metal-catalyzed reactions including allylic substitution [1], Heck reaction [2], hydrogenation [3], hydrosilylation [4] and Diels–Alder reaction [5].

The first highly successful application of these ligands was in the field of Pd-catalyzed enantioselective substitution reactions. Up to 99% ee were achieved starting from racemic 1,3-diphenylpropenyl acetates as substrates. However, selectivities are considerably lower when alkylallyl substrates are used.

The generally accepted mechanism for the palladium-catalyzed allylic substitution is shown in Scheme 1 [6]. In catalytic reactions with phosphinooxazolines the addition of the nucleophile to the cationic [Pd^{II}(η^3-allyl)] intermediate yielding a [Pd^0(η^2-olefin)] complex is considered to be the enantiodetermining step of the reaction [7]. Knowledge of the structures and reactivities

* Corresponding author. Tel.: +41-1-632 4493; fax: +41-1-632 1280

E-mail address: plattner@org.chem.ethz.ch (D.A. Plattner).

0020-1693/02/$ - see front matter
PII: S0020-1693(02)00998-2

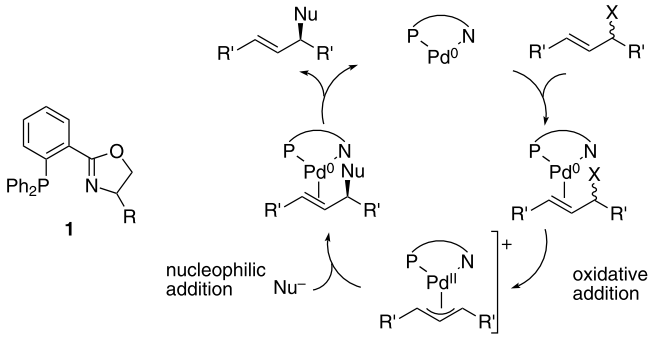

Scheme 1. Catalytic cycle of allylic substitution reaction.

of the intermediates involved in this reaction is crucial for a rationalization of the enantioselectivities observed in allylic substitution. The chemistry of the [Pd(allyl) (**1**)] complexes has been extensively investigated by X-ray analyses and NMR studies [8] and by computional studies [9]. Due to their instability the actual [Pd^0(alkene) (**1**)] intermediates could not be isolated so far. Information was derived from NMR spectroscopy [10] and from [Pd^0(alkene)(P,N)] model complexes with the electron deficient olefins fumarodinitrile [11] and dimethylfumarate [12].

[Pd^{II}(η^3-allyl) (**1**)]PF_6 complexes show dynamic behavior in solution. With [Pd(η^3-PhC_3H_3Ph) (**1**)]PF_6 complexes, in each case two diastereoisomers were found in solution differing in the *exo–endo* orientation of the allyl ligand with respect to the oxazoline moiety [8]. With regard to the orientation of the the allyl substituents only a *syn–syn* arrangement with respect to the central proton was observed. The [Pd(η^3-MeC_3H_3Me) (**1**)]PF_6 derivatives showed also a *syn–anti* isomerization of the allylic substituents.

X-ray analyses revealed that the phosphinooxazoline ligand adopts a rather rigid conformation with the oxazoline substituent in an axial position with respect to the coordination plane. As a consequence, the stereogenic center is remote from the allylic ligand.

In order to bring the chiral information closer to the allylic terminus we synthesized the novel oxazoline ligand **2a** introducing a methyl substituent in α-position to the N atom. The corresponding cationic complexes [Pd^{II}(η^3-PhC_3H_3Ph) (**2a**)]PF_6 (**3a**) and [Pd^{II}(η^3-MeC_3H_3Me) (**2a**)]PF_6 (**4a**) were prepared and their structures were investigated in the solid state and in solution (see Plate 1). A series of [Pd^0(η^2-dmfu)(oxazoline)] complexes (dmfu = dimethylfumarate) was prepared as model compounds for the elusive olefinic intermediates. For comparison, the X-ray structures of complexes [Pd^0(η^2-dmfu) (**2b**)] (**5b**) and [Pd^0(η^2-dmfu) (**1a**)] (**6a**) were added to this account. The efficiency of the novel ligand **2a** was tested in the standard allylic substitution reaction [13].

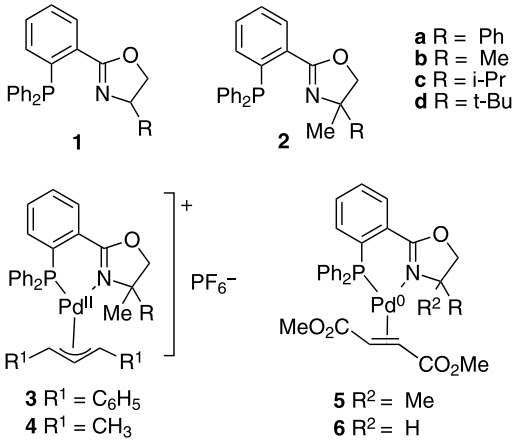

Plate 1.

2. Results

2.1. X-ray structures of allylic complexes

Single crystals of [Pd^{II}(η^3-Ph–C_3H_3–Ph) (**2a**)]PF_6 (**3a**) and [Pd^{II}(η^3-Me–C_3H_3–Me) (**2a**)]PF_6 (**4a**) suitable for X-ray analysis were obtained by crystallization from 1:3:3 CH_2Cl_2–EtOH–hexane. Selected geometrical parameters are reported in Table 1. For numbering see Figs. 1 and 2.

2.1.1. Crystal structure of *3a*

A close similarity of the coordination geometry and of the ligand conformation of **3a** with the [Pd^{II}(η^3-Ph–C_3H_3–Ph) (**1**)] complexes was found. The coordination geometry is pseudo-square-planar. The phosphinooxazoline ligand adopts the characteristic conformation, which has been found in all coordinated phosphinooxazolines of type **1** so far. Due to the non-planarity of the chelate ring one P-phenyl group adopts a pseudo-axial and the other a pseudo-equatorial position. The phenyl substituent of the oxazoline moiety is axially positioned and lies on the same side of the coordination plane as the axial P-phenyl ring. The phenyl substituents of the allyl moiety are in *syn* position with respect to the central proton. The steric interaction between the allyl phenyl group and the oxazoline moiety leads to a

Table 1
Selected bond length (Å) and angles (°) of **3a** and **4a**

	3a	**4a**
Pd–N	2.144(3)	2.118(3)
Pd–P	2.279(1)	2.258(1)
Pd–$C_{cis\,P}$	2.118(3)	2.128(5)
Pd–$C_{central}$	2.204(3)	2.133(5)
Pd–$C_{trans\,P}$	2.365(3)	2.243(5)
N–Pd–P	86.97(8)	88.2(1)
$C_{cis\,P}$–Pd–$C_{trans\,P}$	65.13(12)	68.0(2)
NPdP–CPdC	14.87	10.48

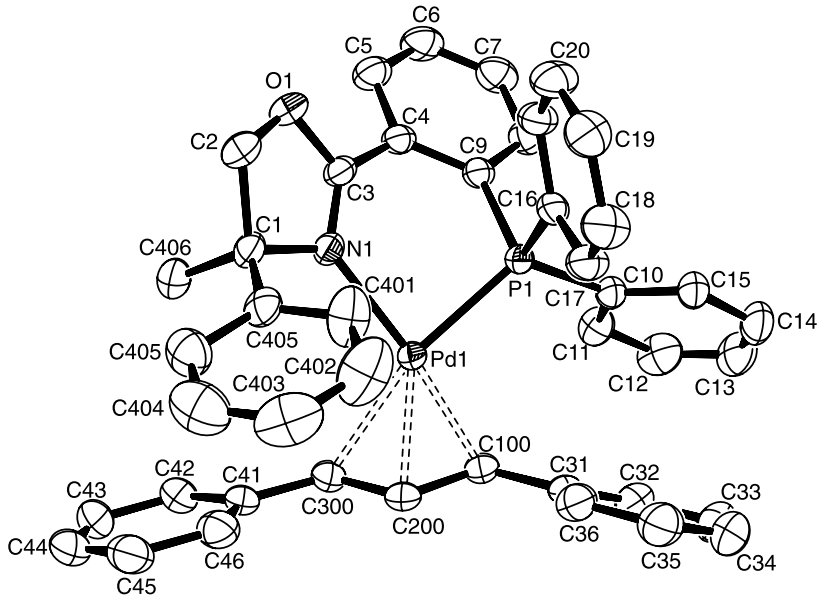

Fig. 1. ORTEP view and labelling scheme of the cation of **3a**. Hydrogen atoms have been omitted. Thermal ellipsoids are drawn at 30% probability.

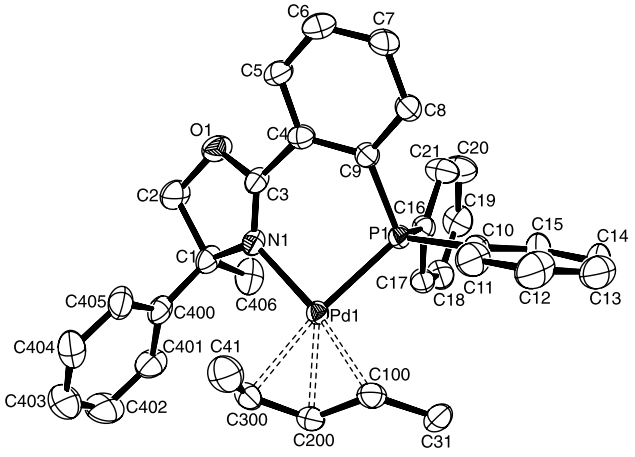

Fig. 2. ORTEP view and labelling scheme of the cation of **4a**. Hydrogen atoms have been omitted. Thermal ellipsoids are drawn at 30% probability.

distortion of the square-planar coordination geometry. The Pd–P–N plane forms an angle of 14.9° with the Pd–C(100)–C(300) plane.

2.1.2. Crystal structure of *4a*

The coordination geometry of **4a** is pseudo-square-planar. The overall geometry of complex **4a** differs substantially from that of **3a**. The allyl group adopts exclusively *syn–anti* configuration, with the allylic methyl substituent *cis* to the oxazoline moiety in *anti* position. The backbone of the phosphinooxazoline ligand is pseudo-enantiomeric to that of **3a**. The phenyl substituent at the stereogenic center is pseudo-equatorially positioned with respect to the Pd–P–N plane. It lies in the coordination plane close to the adjacent allyl terminus. The allyl substituent *cis* to the phosphine moiety is situated in the groove between the P-phenyl rings. Studies by Pregosin and Albinati confirmed that this arrangement of the PPh_2 moiety and the allyl substituent is sterically favored [14].

2.2. Crystal structures of olefinic complexes

Crystals of [Pd^0(η^2-$MeO_2C{=}CO_2Me$) (**2b**)] (**5b**) and of [Pd^0(η^2-$MeO_2C{=}CO_2Me$) (**1a**)] (**6a**) were obtained by slow diffusion of pentane into a saturated Et_2O–CH_2Cl_2 solution. Selected geometrical parameters are reported in Table 2. For numbering see Figs. 3 and 4.

2.2.1. Crystal structure of *5b*

Crystals of **5b** contain two crystallographically independent molecules per asymmetric unit. One molecule is disordered in the chelate ring portion. The second molecule shows no signs of disorder and is depicted in Fig. 3. Except for disorder a close similarity of the two molecules is observed. The alkene ligand is in a sterically

Table 2
Selected bond length (Å) and angles (°) for **5b** and **6a**

	5b (**1**)	**5b** (**2**)	**6a**
Pd–N	2.161 (4)	2.162 (7)	2.143 (3)
Pd–P	2.268 (1)	2.266 (1)	2.267 (1)
Pd–$C_{cis\,P}$	2.057 (4)	2.061 (4)	2.067 (3)
Pd–$C_{trans\,P}$	2.117 (5)	2.137 (4)	2.108 (4)
C–C	1.414 (8)	1.427 (8)	1.399 (5)
N–Pd–P	85.8 (1)	84.2 (4)	84.9 (1)
C–Pd–C	39.6 (2)	39.7 (2)	39.2 (2)
C–C=C–C	148.6	151.6	150.1
NPdP–CPdC	6.25	7.62	17.80

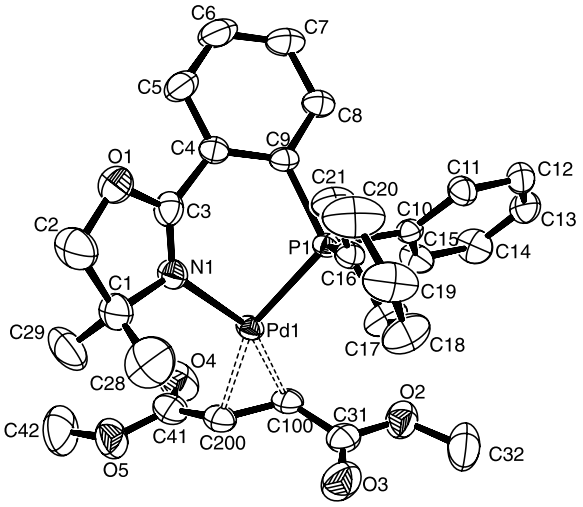

Fig. 3. ORTEP view and labelling scheme of **5b**. Hydrogen atoms have been omitted. Thermal ellipsoids are drawn at 30% probability. For clarity only the not disorderd molecule is shown.

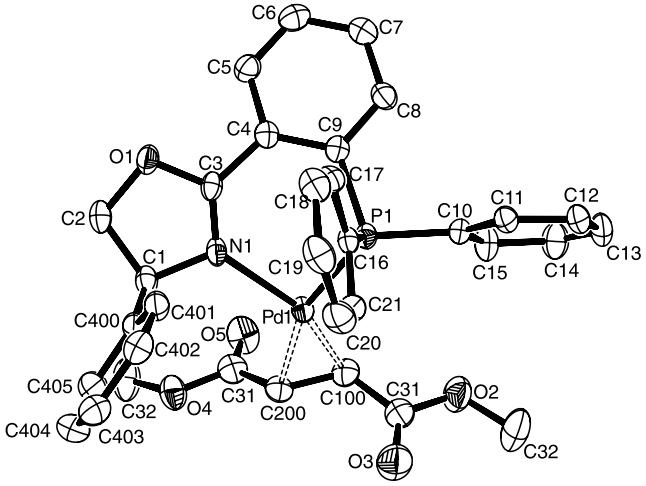

Fig. 4. ORTEP view and labelling scheme of **5b**. Hydrogen atoms have been omitted. Thermal ellipsoids are drawn at 30% probability.

favorable orientation. The CO_2Me group *cis* to the phosphine moiety lies between P-phenyl rings, the CO_2Me substituent *cis* to the oxazoline moiety is remote from the oxazoline substituents.

The coordination geometry is trigonal. The C=C bond of the alkene ligand is positioned approximately in the N–Pd–P coordination plane. Bond lengths and angles of the coordination sphere are in the expected range. Due to the *trans* influence of the phosphine group, the Pd–C distance *trans* to *P* is longer than that *trans* to *N*.

2.2.2. Crystal structure of **6a**

A close similarity with complex **5b** is found. The oxazoline ligand adopts the characteristic conformation of coordinated phosphinoxazolines of type **1**. The CO_2Me group adjacent to the oxazoline moiety is remote from the oxazoline substituent. The steric strain leads to a rotation of the olefinic bond out of the Pd–P–N plane.

The alkene ligand is not planar. The C–CO_2Me and C–H bonds are bent away from the palladium center. The C–C=C–C torsion angle is about 150°. The length of the C=C bond of 1.39 Å is significantly greater than that for the free olefin (1.36 Å). Both the deviation from planarity and the elongation of the olefin bond provide evidence of a partial sp^3-hybridization of the olefinic carbons.

2.3. NMR spectroscopy of allylic compounds

Selected NMR data are listed in Table 3.

2.3.1. NMR spectroscopy of **3a**

The NMR spectra of **3a** suggest that two isomers are present in solution. According to the J_{HH} coupling constants of the allyl protons the phenyl substituents of the major component (84%) are in the *syn* position relative to the central proton. The chemical shift of the central proton gives evidence that the oxazoline adopts the same conformation in solution as in the solid state: The shielding effect of the axially positioned phenyl substituent at the oxazoline moiety shifts the resonances of the central allyl proton of the *exo* isomer to higher field (5.80 ppm) relative to the corresponding signal of the *endo* isomer ($\sim$7 ppm). A highfield shift of the $H_{trans\,P}$ resonance of the minor isomers suggests the *endo–syn–syn* structure.

2.3.2. NMR spectroscopy of **4a**

According to the ^{31}P NMR spectrum at least six isomers exist in $CDCl_3$ solution. These arise from *exo–endo* orientation of the allyl group and *syn–syn* or *syn–anti* positions of the allyl substituents. In addition, the phosphinooxazoline moiety may flip between two conformations. The ^1H NMR shifts were assigned to isomers I–IV (Fig. 5). The signals of isomers V and VI are hidden and too small for an unambiguous assignment. The orientation of the allyl substituents was determined on the basis of the coupling patterns. The coupling constant $^4J_{HP}$ of a *syn* methyl group is larger (ca. 10 Hz) than that of an *anti* methyl group (ca. 6 Hz). The conformation of the oxazoline and the orientation of the allyl group were derived from the high field shifts of resonances of the allyl ligand due to the anisotropic ring current effect of the oxazoline phenyl ring. An axially positioned phenyl ring is situated above the allyl group and causes an upfield shift of the resonance of the central proton of the *exo* isomers. In *endo* isomers, the axially positioned phenyl ring affects the resonances of the adjacent terminal *anti* proton or methyl substituent, respectively. An equatorial phenyl group is close to the allyl terminus and influences both the $H_{trans\,P}$ and the

Table 3
Selected ^{1}H NMR chemical shifts (δ ppm) of **3a** and **4a** with coupling constants (J Hz) in parentheses in comparison with those of **4b** [8e]

	Isomer	Percentage	$Me_{cis\,P}$	$Me_{trans\,P}$	$H_{cis\,P}$	$H_{central}$	$H_{trans\,P}$	^{31}P
3a	I	84			3.96 [a]	5.80 (10.5,13.9)	6.33 [a]	21.33
	II	16			4.33 [a]	6.33 [a]	4.71 (11.7,12.5)	25.87
4a	I	11	0.75 [a]	0.88 [a]	3.39 [a]	4.89 (~ 12)	4.53 [a]	23.85
	II	15	0.73–0.78 [a]	0.72–0.78 [a]	3.20 (6.2, 13.3)	5.39 (11.0, 13.3)	4.15 [a]	22.00
	III	20	0.91 (6.2, 9.3)	1.29 (6.7, 6.7)	3.55 [a]	4.35 [a]	5.13 [a]	24.76
	IV	47	0.97 (6.2, 9.6)	0.70 (6.7, 6.7)	3.55 (6.2, 11.9)	5.28 (8.4, 11.9)	4.12 [a]	23.73
	V	4	[a]	[a]	[a]	[a]	[a]	19.61
	VI	3	[a]	[a]	[a]	[a]	[a]	18.98
4b	I	33	0.83 (6.3, 11.3)	1.88 (6.0,11.5)	3.41 (6.3, 10.6)	5.53 (11.5, 12.4)	4.8 [a]	24.32
	III	50	1.02 (6.3, 9.8)	1.35 (6.3,6.9)	3.74 (6.3, 12.1)	5.60 (8.7, 12.1)	5.95 (~ 7)	25.82
	V	17	1.19 (~ 7.7)	1.90 [a]	3.95 (6.7, 7.7)	5.56 [a]	4.8 [a]	20.30

[a] Chemical shift and/or coupling constants not determined due to signal overlap.

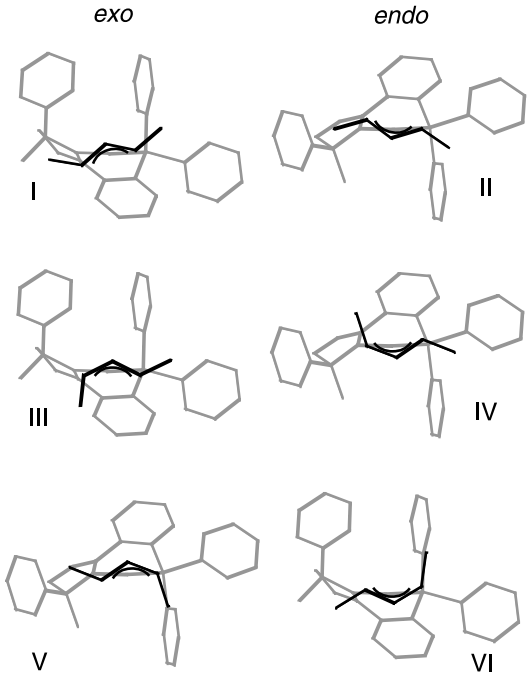

Fig. 5. Diastereoisomers of **4a** in $CDCl_3$ solution. (*Exo*: the central C–H bond of the allyl group points towards the larger substituent R; *endo*: the central C–H bond points away from the larger substituent).

$Me_{trans\,P}$ signals but not the chemical shift of the $H_{central}$ resonance, irrespective of the orientation of the ligand.

Following this scheme, the NMR data suggest that the main isomer (isomer IV) has the same structure as found in the solid state (highfield shift of the $Me_{trans\,P}$ and $H_{trans\,P}$ resonance). In contrast, the highfield shift of the $H_{central}$ resonance of isomers I and III in comparison with that of II and IV suggests an axial position of the oxazoline phenyl ring.

2.4. NMR spectroscopy of olefinic complexes

Selected NMR data are listed in Table 4 (for a representation of isomers M and m, see Plate 2). Complexes of type **5** and **6** with chiral ligands exist in solution as a mixture of two diastereoisomers, which differ in the orientation of the alkene group with respect to the oxazoline ligand. Only one isomer is found for **5b**.

The signals are assigned according to the J_{PH} coupling constants, expected to be larger for *trans* than for *cis* coupling. The orientation of the dimethylfumarate ligand and the conformation of the oxazoline ligand of **5a** and **6a** were derived from the highfield shift of the resonances of the alkene proton and the protons of the methyl group *trans* to *P* in analogy to the allylic complexes.

2.4.1. Spectrum of *5a*

According to the highfield shift of the $H_{trans\,P}$ resonance (3.04 vs. 3.8 ppm) the alkene ligand has the same orientation with respect to the phosphinooxazoline as observed in the solid state structures of **5b** and **6a**. In the minor isomer, a significant highfield shift of the $Me_{trans\,P}$ resonance (2.87 vs. 3.6 ppm) is observed. As the $Me_{trans\,P}$ resonance (3.55 vs. 3.6 ppm) of the major diastereoisomer as well as the $H_{trans\,P}$ resonance (3.57 vs. 3.69 ppm) of the minor isomer are not significantly affected, it can savely be assumed that the oxazoline moiety adopts the same conformation as ligands of type **1** with the phenyl ring axially positioned. There is no evidence of a flipping of the chelate ring.

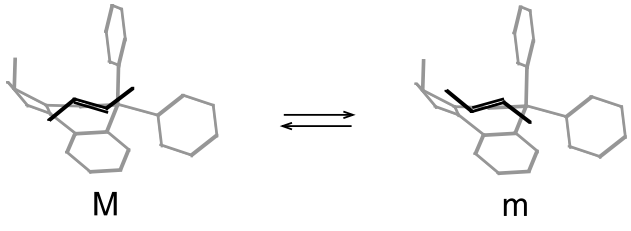

Plate 2.

Table 4
Selected ^{1}H NMR chemical shifts (δ ppm) of **5a**, **5b** and **6a**–**6d** with coupling constants (J Hz) in parentheses

	Isomer	Percentage	H–C$_{cis\,P}$ (J_{HH}, J_{HP})	H–C$_{trans\,P}$ ($J_{HH} \sim J_{HP}$)	Me$_{cis\,P}$	Me$_{trans\,P}$ (J_{HP})	^{31}P(H)
5a	M	67	dd 3.98 (10.1, 2.1)	pt 3.04 (10.1)	s 3.03	s 3.55 (0.8)	20.20
	m	33	dd 4.03	pt 3.55	s 3.17	s 2.87 (0.8)	20.09
5b	M		dd 4.14 (10.0, 2.3)	pt 3.81 (10.2)	s 3.11	d 3.58 (0.9)	21.59
6a	M	72	dd 4.07 (10.3, 1.8)	dd, 3.39 (10.3, 10.8)	s 2.99	d 3.65 (0.7)	20.18
	M	28	dd 4.02 (10.1, 2.4)	pt 3.69 (10.1)	s 3.37	d 2.92 (0.7)	20.23
6b	M	54	dd 4.15 (10.1, 0.7)	pt 3.93 (10.2)	s 3.07	d 3.59 (0.5)	20.25
	M	46	dd 4.17 (10.1, 0.9)	pt 3.78 (10.1)	s 3.32	d 3.61 (0.5)	21.44
6c	M	62	[a]	pt 3.91 (10.4)	s 3.06	s 3.60	19.89
	M	38	[a]	pt 3.74 (10.4)	s 3.33	s 3.60	20.87
6d	M	80	4.21 [a]	pt 3.79 (10.4)	s 3.10	d 3.60 (0.8)	20.95
	M	20	4.21 [a]	pt 3.79 [a]	s 3.50	d 3.61 (0.8)	21.62

s, singlet; d, doublet; pt pseudo-triplet.

2.4.2. Spectra of **5c** and **6b–d**

The chemical shifts of the alkene groups in these complexes display a close similarity. The signal of the proton *cis* to P ($J_{PH} \sim 2$) appears in the range of 4.0–4.2 ppm. The pseudo-triplet of the protons *trans* to P ($J_{PH} \sim 10$) appears at approximately 3.8 ppm. In general, the signal of the methyl protons *trans* to P appears at 3.6 ppm as a narrow doublet due to a long range coupling to the phosphorus ($J_{PH} < 1$ Hz). The resonance of the methyl protons *cis* to P of the main isomers appears at $\sim$3.1 ppm, that of the minor one at $\sim$3.3 ppm. This suggests that the major isomers adopt conformation M in all complexes.

2.4.3. Spectrum of **6a**

According to the highfield shift of the H$_{trans\,P}$ resonance (3.39 vs. 3.8 ppm) the major isomer has the same structure as that found in the solid state. In the minor diastereoisomer, the highfield shift of the Me$_{trans\,P}$ resonance (2.92 vs. 3.6 ppm) is consistent with a structure with opposite orientation of the alkene group.

2.5. Enantioselective allylic substitution

Asymmetric allylic substitution of the allyl acetates **7** and **8** with dimethyl malonate was carried out with catalyst **2a** following the method with *N*,*O*-bis(trimethylsilyl)acetamide (BSA) under the same conditions as with ligands **1** (Scheme 2) [13]. The results of the catalysis are listed in Tables 5 and 6.

The reaction of allyl acetate rac.-**7** with the malonic ester nucleophile led to the formation of the chiral non

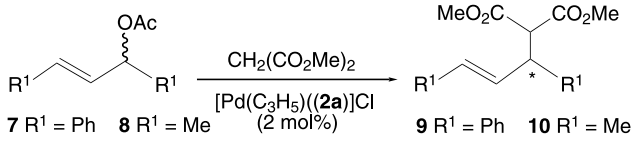

Scheme 2. Enantioselective allylic substitution reaction.

Table 5
Asymmetric induction of ligand **2a** in comparison with that of ligands of type **1** [1a]

L	Substrate	Yield (%)	ee (%)	Product
(*S*)-**2a**	Rac.-**7**	77	97	(*S*)-**9**
(*S*)-**1a**	Rac.-**7**	99	99	(*S*)-**9**
(*S*)-**2a**	Rac.-**8**	93	18	(*S*)-**10**
(*S*)-**1a**	Rac.-**8**	97	50	(*S*)-**10**
(S)-**1b**	Rac.-**8**	95	56	(*S*)-**10**
(*S*)-**1c**	Rac.-**8**	99	59	(*S*)-**10**
(*S*)-**1d**	Rac.-**8**	96	71	(*S*)-**10**

racemic product (*S*)-**9** with a high enantioselectivity (97%) comparable with that induced by ligands of type **1**. For the alkylallyl acetate **8** the enantioselectvity was dramatically lower with ligand **2a** (18%). With ligands of type **1** the enantiomeric excess is higher than for **2a** but only moderate (50–71%).

For the diphenylallyl acetates **7**, the stereochemical course of the allylic substitution reaction may be rationalized as proposed in Ref. [6](b). Nucleophilic attack at the strongly favored isomer I leads to the favored Pd(olefin) complex (*S*)-M (Scheme 3). Nucleophilic attack at the minor isomer II leads to the disfavored olefinic diastereoisomer (*R*)-m. As a consequence, a high enantioselectivitiy results.

An analysis of the equilibria of the (dimethylallyl)palladium complexes and the relative stabilities of the (olefin)palladium complexes derived from the isomeric ratios of the palladium(dimethylfumarate) complexes gives insight into the origin of enantioselection. It has been generally accepted that the nuclephilic attack takes place at the weaker bound allyl terminus *trans* to P [6](b). Neglecting nucleophilic attack *cis* to *P* and diastereoisomers leading to *Z*-isomers, the allylic intermediates I–IV are involved in the catalytic reaction. Nucleophilic attack at the allyl terminus *trans* to P leads to four Pd(olefin) diastereoisomers, differing in the

Table 6
Isomeric ratio of [Pd(dimethylallyl)(oxazoline)] and the [Pd(dmfu)(oxazoline)] complexes vs. asymmetric induction

	[Pd(dimethylallyl)(oxazoline)]	[Pd(dmfu)(oxazoline)	Catalysis
	Ratio of isomers involved in catalytic reaction (%) **I**:**II**:**III**:**IV** (de_S)	Ratio of isomers (%) M:m	ee (%)
2a	11:16:22:51 (24)	67:33	18
1a	50:31:19 (0) [a]	72:28	50 [b]
1b	75:16:9 (50) [a]	54:46	56 [b]
1c	74:18:8 (48) [a]	62:38	59 [b]
1d	72:15:13 (44) [a]	80:20	71 [b]

(de_S) diastereomeric excess of isomers leading to *S*-**10**.
[a] obtained from Ref. [8e].
[b] obtained from Ref. [1a].

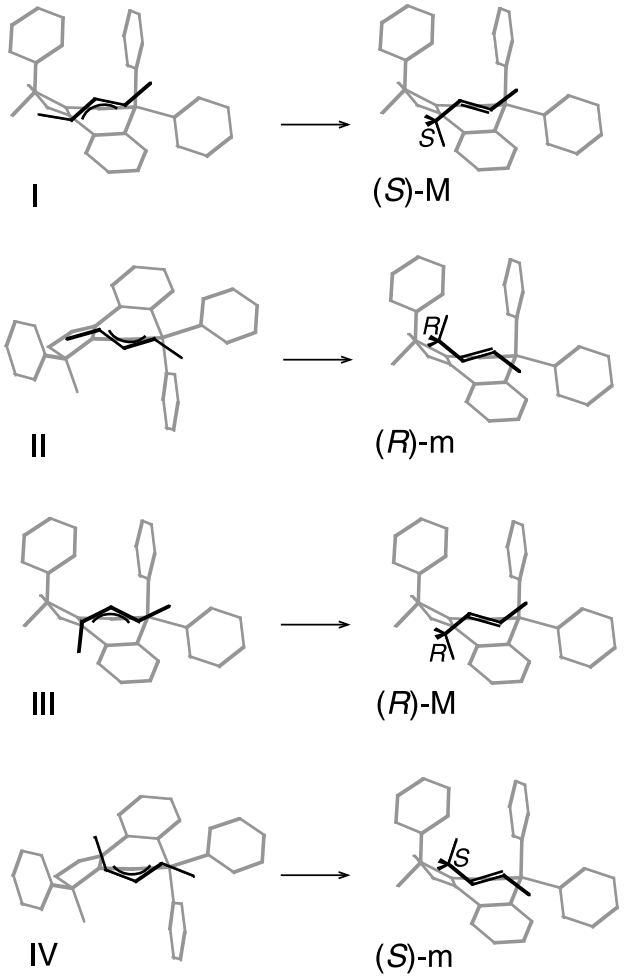

Scheme 3. Intermediates in allylic substitution reaction.

orientation of the olefin moiety with respect to the oxazoline ligand and in the configuration of the stereogenic center, respectively.

In the catalytic reaction with 1-methylbut-2-enyl acetate **8** and ligand **2a** isomers I and IV lead to the (*S*)-configured product, the major enantiomer in the catalytic reaction. The main isomer is diastereoisomer IV. Nucleophilic attack at the allyl terminus of this isomer leads to the disfavored olefinic product (*S*)-m. A decrease of the asymmetric induction with respect to the diastereoisomer ratio is observed.

For ligands of type **1** isomers I–III are involved in the formation of product **10**. Isomer IV was not detectable in solution. For the phenyl derivative **1a**, an equal abundance of isomers leading to (*S*)-**10** or (*R*)-**10**, respectively, was detected by NMR spectroscopy. With respect to the olefin complexes, however, the isomer (*S*)-M derived from isomer I leading to (*S*)-**10** is clearly favored, thus a respectable ee of 50% results.

For ligands **1b**–**d**, an almost equal abundance of the major Pd(η^3-allyl) isomer I was found. A comparison of the diastereomeric ratios of complexes **6** reveals that the stability of the major Pd(η^2-olefin) isomer M relative to that of the minor isomer m increases with the bulk of the oxazoline substituent. The methyl derivative **1b** induces a poor discrimination between the major and minor isomer. As a consequence, the enantiomeric excess induced by **1b** is only marginally higher (56%) than the diastereomeric excess of the allylic isomer I (50%). In contrast, the major isomer of the t-butyl derivative is clearly favored (M:m = 80:20). In spite of a lower diastereomeric excess of the [Pd(η^3-allyl)] isomer I (44%) ligand **1d** induces an enantioselectivity of 71%. The results give evidence that the enantiomeric excess is strongly correlated with the relative stabilities of the diastereomeric olefin complexes. The influence of the relative concentrations of the allylic intermediates on the enantioselectivity of the catalytic reaction is much lower, but is observable.

3. Conclusion

The enantioselectivity induced by ligand **2a** in the enantioselective allylic substitution reaction is in the same range as that obtained with the analogous ligands of type **1** using 1,3-diphenylprop-2-enyl acetate as substrate. With 1-methylbut-2-enyl acetate the enantiomeric excess obtained with ligand **2a** is drastically lower in comparison with that of ligands of type **1**. Investiga-

tion of the (dimethylallyl)palladium intermediates and the corresponding olefinic (dmfu)palladium complexes suggests that the moderate selectivity is due to the conformational lability of ligand **2a** leading to preferential formation of (allyl)palladium species other than the *exo–syn–syn* diastereoisomer. These either lead to the formation of the product of opposite chirality (II and III) or are less reactive due to an unfavorable transition state (IV).

A comparison of the isomeric ratios of the [Pd(dimethylallyl) (**1**)] and the [Pd(dmfu) (**1**)] complexes versus the degree of asymmetric induction demonstrates a strong correlation between the relative stabilities of the olefinic intermediates and the asymmetric induction. The relationship between the relative concentrations of the allylic intermediates and the enantiomeric excess is less pronounced but clearly observable.

4. Experimental

4.1. General

$Pd_2(dba)_3 \cdot CHCl_3$ [15], racemic α-methylphenylglycine [16] and enantiomerically pure α-methylphenylglycine [17] were prepared according to literature procedures. Preparation of ligands **1a**–**d** and **2b** is described in [18]. The solvents for chromatography were distilled before use. The reactions were carried out under N_2 using dried glassware. Column chromatography (CC): SiO_2, C 560, 0.035–0.070 mm, F 254, Chemische Fabrik, Uetikon. When not stated otherwise, NMR spectra were recorded at room temperature (r.t.) on a Varian–Gemini 300 spectrometer with $CDCl_3$ as solvent; ^1H NMR: 300 MHz, chemical shifts in ppm relative to $CHCl_3$ as internal reference (7.26 ppm), coupling constants J in Hz; $^{31}P\{^1H\}$ NMR: 121 MHz, triphenyl phosphate as external reference (−18.0 ppm).

4.2. Preparation of ligand *2a*

4.2.1. α-Methylgycinol

α-Methylphenylglycine (0.3 g, 1.8 mmol) was added to a stirred suspension of $NaBH_4$ (0.3 g, 8.1 mmol) in THF (10 ml). The reaction mixture was immersed in an ice bath and a solution of concentrated H_2SO_4 (0.18 ml) in Et_2O (0.42 ml) was added dropwise. The stirring was continued at r.t. overnight. MeOH (1 ml) and 5 N NaOH (10 ml) were successively added. After removing the organic solvents, the aqueous solution was refluxed for 2 h and, after cooling, extracted with CH_2Cl_2. Evaporation of the solvent yielded α-methylgycinol (0.18 g, 81%) as a colorless solid. ^1H NMR ($CDCl_3$): δ 1.43 (s, 3H, CH_3), 2.21 (s (br), 3H, OH, NH), 3.54 (d, 1H, $J = 10.8$, CH_2) 3.62 (d, 1H, $J = 10.8$, CH_2), 7.24–7.44 (m, 5H, arom).

4.2.2. 2-[2′-(Diphenylphosphino)phenyl]-4,5-dihydro-4-methyl-4-phenyloxazole (*2a*)

α-Phenylglycinol (0.18 g, 1.2 mmol), cyanophenyl(diphenyl)phosphine (0.32 g, 1.1 mmol) and $ZnCl_2$ (0.17 g, 1.3 mmol) under N_2 were heated to reflux for 94 h. The mixture was submitted to CC (4 × 5 cm, silica-gel). The unreacted benzonitrile was removed with 1:2 CH_2Cl_2–hexane (50 ml). A mixture of **2a** and [Zn (**2a**)Cl_2] was eluted with AcOEt and isolated as a colorless solid (0.42 g). The mixture was dissolved in $CHCl_3$ (3 ml) and treated with 2,2′-bipyridine (0.14 g, 0.9 mmol) in $CHCl_3$ (2 ml). The resulting suspension was stirred for 30 min and submitted to CC (2 × 3 cm, silica-gel, ($CHCl_3$ 100 ml)). A colorless solid resulted (0.32 g, 68.4%). ^1H NMR ($CDCl_3$): 1.35 (s, 3H, CH_3), 4.15, 4.20 (2 d, 2H, $J = 8.0$, CH_2), 6.87–6.92 (m, 1H, arom), 7.14–7.40 (m, 19 H, arom), 7.95–7.80 (m, 1H, arom).

4.3. Preparation of allylic compounds

A mixture of 1 equiv. of the $[(allyl)PdCl]_2$ dimer and of 2.1 equiv. of phopshinooxazoline was stirred in EtOH for 15 min. The resulting solution was treated with 3 equiv. of NH_4PF_6. After 10 min the complexes were filtered off and recrystallized from CH_2Cl_2–EtOH–hexane.

4.3.1. (η^3-1,3-diphenylallyl){2-[2′-(diphenylphosphino)phenyl]-4,5-dihydro-4-methyl-4-phenyloxazole}palladium(II) hexafluorophosphate (*3a*)

Yield: 76%. Recrystallization from CH_2Cl_2–EtOH–hexane 1:3:3 afforded air-stable crystals suitable for X-ray analysis.

^1H NMR ($CDCl_3$, r.t.): major isomer (84%): δ 0.92 (s, 3H, Me), 3.96 (d, 1H, $J = 8.9$, CH_2), 3.96 (d, 1H, $H_{cis\,P}$), 4.37 (d, 1H, $J = 8.9$, CH_2), 5.80 (dd, 1H, $J = 11.7$, 12.5, $H_{central}$), 6.27–6.37 (m, 3H, arom, $H_{trans\,P}$), 7.35–7.73 (m, 21H, arom), 8.04–8.09 (m, 1H, arom). $^{31}P\{H\}$ NMR: 21.33.

Minor isomer (16%): δ 1.31 (s, 3H, Me), 4.03, 4.11 (2d, 2H, $J = 8.6$, CH_2), 4.33 (d, 1H, $H_{cis\,P}$), 4.71 (dd, 1H, $J = 10.5$, 13.0, $H_{trans\,P}$), 6.27–6.37 (m, 3H, arom, $H_{central}$), 7.35–7.73 (m, 21H, arom), 7.96–8.00 (m, 1H, arom). $^{31}P\{H\}$ NMR: 25.87.

4.3.2. (η^3-1,3-dimethylallyl){2-[2′-(diphenylphosphino)phenyl]-4,5-dihydro-4-methyl-4-phenyloxazole}palladium(II) hexafluorophosphate (*4a*)

Yield: (82%). Recrystallizing from CH_2Cl_2–EtOH–hexane 1:3:3 afforded crystals suitable for X-ray analysis containig 1 equiv. of CH_2Cl_2.

^1H NMR (400 MHz, $CDCl_3$, r.t.): major isomer (isomer IV): δ 0.70 (pt, 3H, $J_{HH}-J_{HP} = 6.7$, $Me_{trans\,P}$), 0.97 (dd, 3H, $J_{HH} = 6.2$, $J_{HP} = 9.6$, $Me_{cis\,P}$), 1.51 (s, 1H, Me), 3.55 (dq, 1H, $J = 6.2$, 11.9, $H_{cis\,P}$), 4.12 (ddq, 1H, $H_{trans\,P}$), 4.30, 4.59 (2 d, 2H, $J = 9.0$, CH_2), 5.28 (dd, 1H,

$J = 8.4$, 11.9, $H_{centr.}$), 7.21–7.78 (m, 13H, arom), 8.20–8.60 (m, 1H, arom).

Isomer I: δ 0.75 (3H, $Me_{cis\,P}$), 0.88 (3H, $Me_{trans\,P}$), 1.85 (3H, Me), 3.39 (1H, $H_{cis\,P}$), 4.53 (1H, $H_{trans\,P}$), 4.89 (pt, 1H, J–12, $H_{central}$), 7.21–7.78 (m, 13 H, arom), 8.00–8.05 (m, 1H, arom).

Isomer II: δ 0.75 (2dd, 6H, $Me_{cis\,P}$, $Me_{trans\,P}$), 1.71 (s, 1H, Me), 3.20 (dq, 1H, $J = 6.2$, 13.3, $H_{cis\,P}$), 4.15 (ddq, 1H, $H_{trans\,P}$), 5.39 (dd, 1H, $J = 11.0$, 13.3, $H_{central}$), 7.21–7.78 (m, 13 H, arom), 8.00–8.05 (m, 1H, arom).

Isomer III: δ 0.91 (dd, 3H, $J_{HH} = 6.2$, $J_{HP} = 9.3$, $Me_{cis\,P}$), 1.29 (pt, J_{HH}–$J_{HP} = 6.7$, 3H, $Me_{trans\,P}$), 1.96 (s, 3H, Me), 3.55 (dq, 1H, $H_{cis\,P}$), 4.21, 4.73 (2 d, 2H, $J =$ 9.1, CH_2), 4.35 (dd, 1H, H_{centr}), 5.13 (ddq, 1H, $H_{trans\,P}$), 6.97–7.00 (m, 2H, arom), 7.21–7.78 (m, 11H, arom), 8.00–8.05 (m, 1H, arom).

The synthesis and characterization of the [Pd(dimethylallyl)(**1**)] complexes is described elsewhere [8e].

4.4. Preparation of [Pd(η^2-dimethylfumarate)(oxazoline)] complexes

A solution of 1 equiv. of $Pd_2(dba)_3 \cdot CHCl_3$ and 2.1 equiv. of the oxazoline ligand in CH_2Cl_2 was stirred for 30 min at r.t. until the dark purple solution turned dark brown. Subsequently 2.5 equiv. of dimethylfumarate was added. The mixture was stirred for 2 h finally turning yellow. The solution was concentrated and transferred onto a SiO_2 column and eluted with 2:1 hexane–AcOEt. Evaporation of the solvent yielded the dimethylfumarato complexes as yellow solids.

4.4.1. (η^2-dimethylfumarate){2-[2′-(diphenylphosphino)phenyl]-4,5-dihydro-4-methyl-4-phenyloxazole]}palladium(0) (**5a**)

Yield: 40%.

^{1}H NMR: major isomer: δ 1.78 (s, 3H, Me), 3.03 (s, 3H, $Me_{cis\,P}$), 3.04 (pt, J_{HH}–$J_{HP} = 10.1$, 1H, $H_{trans\,P}$), 3.55 (d, 3H, $J_{HP} = 0.85$, $Me_{trans\,P}$), 3.98 (dd, $J_{HH} = 10.1$, $J_{HP} = 2.1$, 1H, $H_{cis\,P}$), 4.30, 4.41 (2 d, $J = 8.6$, 2H, CH_2), 6.86–7.71 (m, 18H, arom), 8.02–8.07 (m, 1H, arom). ^{31}P{H} NMR: δ 20.20.

Minor isomer: δ 1.94 (s, 3H, Me), 2.87 (d, 3H, $J_{HP} =$ 0.8, $Me_{trans\,P}$), 3.17 (s, 3H, $Me_{cis\,P}$), 3.55 (pt, 1H, $H_{trans\,P}$), 6.86–7.71 (m, 18H, arom), 8.15–8.20 (m, 1H, arom). ^{31}P{H} NMR: δ 20.09.

4.4.2. (η^2-dimethylfumarate){4,4-dimethyl-2-[2′-(diphenylphosphino)phenyl]-4,5-dihydrooxazole]}palladium(0) (**5b**)

Yield: 40%. Diffusion of pentane into a saturated Et_2O–pentane–CH_2Cl_2 solution yielded crystals suitable for X-ray analysis.

^{1}H NMR: δ 1,20, 1.30 (2 s, 6H, Me), 3.11 (s, 3H, $Me_{cis\,P}$), 3.58 (d, 3H, $J_{HP} = 0.9$, $Me_{trans\,P}$), 3.81 (pt, J_{HH}–$J_{HP} = 10.2$, 1H, $H_{trans\,P}$), 3.98, 4.08 (d, $J = 8.3$, 2H, CH_2), 4.14 (dd, $J_{HH} = 10.0$, $J_{HP} = 2.3$, 1H, $H_{cis\,P}$), 6.89–6.95 (m, 1H, arom), 7.20–7.52 (m, 12H, arom), 7.89–7.93 (m, 1H, arom). ^{31}P{H} NMR: δ 21.59.

4.4.3. (η^2-dimethylfumarate){2-[2′-(diphenylphosphino)phenyl]-4,5-dihydro-4-phenyloxazole]} palladium(0) (**6a**)

Yield: 64%. Diffusion of pentane into a saturated Et_2O–pentane–CH_2Cl_2 solution yielded crystals suitable for X-ray analysis.

^{1}H NMR: major isomer: δ 2.99 (s, 3H, $Me_{cis\,P}$), 3.39 (dd, 1H, $J_{HH} = 10.3$, $J_{HP} = 10.8$, $H_{trans\,P}$), 3.65 (d, 3H, $J = 0.71$, $Me_{trans\,P}$), 4.07 (dd, 1H, $J_{HH} = 10.3$, $J_{HP} = 1.8$, $H_{cis\,P}$), 4.24 (dd, 1H, $J = 7.9$, 8.7, CH_2), 4.76 (dd, 1H, $J = 8.7$, 10.5, CH_2), 5.43 (dd, 1H, $J = 7.9$, 10.5, CH), 6.92–7.53 (m, 18H, arom), 8.10–8.14 (m, 1H, arom). ^{31}P{H} NMR: δ 20.19.

Minor isomer: δ 2.92 (d, 3H, $J = 0.7$, $Me_{trans\,P}$), 3.37 (s, 3H, $Me_{cis\,P}$), 3.69 (pt, 1H, $J_{HH} = J_{HP} = 10.1$, $H_{trans\,P}$), 4.02 (dd, 1H, $J_{HH} = 10.1$, $J_{HP} = 2.8$, $H_{cis\,P}$), 4.24 (dd, 1H, $J = 5.0$, 8.4, CH_2), 4.71 (dd, 1H, $J = 8.4$, 10.1, CH_2), 5.70 (dd, 1H, $J = 5.0$, 10.1, CH), 6.81–7.53 (m, 18H, arom), 8.15–8.19 (m, 1H, arom). ^{31}P{H} NMR: δ 20.23.

4.4.4. (η^2-dimethylfumarate){2-[2′-(diphenylphosphino)phenyl]-4,5-dihydro-4-methyl-oxazole]}palladium(0) (**6b**)

Yield: 62%.

^{1}H NMR: major isomer: δ 1.33, (d, 3H, $J = 6.5$, Me), 3.07 (s, 3H, $Me_{cis\,P}$), 3.59 (d, 3H, $J_{HP} = 0.5$, $Me_{trans\,P}$), 3.93 (pt, J_{HH}–$J_{HP} = 10.2$, 1H, $H_{trans\,P}$), 3.95–4.01 (m, 1H), 4.15 (dd, $J_{HH} = 10.1$, $J_{HP} = 0.7$, 1H, $H_{cis\,P}$), 4.33–4.48 (m, 2H), 7.06–7.11 (m, 1H, arom), 7.20–7.52 (m, 12H, arom), 8.00–8.06 (m, 1H, arom). ^{31}P{H} NMR: δ 20.25.

Minor isomer: δ 1.04, (d, 3H, $J = 6.4$, Me), 3.32 (s, 3H, $Me_{cis\,P}$), 3.61 (d, 3H, $J_{HP} = 0.8$, $Me_{trans\,P}$), 3.76 (pt, J_{HH}–$J_{HP} = 10.1$, 1H, $H_{trans\,P}$), 3.95–4.01 (m, 1H), 4.17 (dd, $J_{HH} = 10.1$, $J_{HP} = 0.9$, 1H, $H_{cis\,P}$), 4.33–4.48 (m, 2H), 6.94–6.99 (m, 1H, arom), 7.20–7.52 (m, 12H, arom), 7.97–8.00 (m, 1H, arom). ^{31}P{H} NMR: δ 21.44.

4.4.5. (η^2-dimethylfumarate){2-[2′-(diphenylphosphino)phenyl]-4,5-dihydro-4-isopropyloxazole]}palladium(0) (**6c**)

Yield: 51%.

^{1}H NMR: major isomer: δ 0.32 (d, 3H, $J = 6.9$, Me), 0.81–0.90 (d, 3H, Me), 2.42–2.54 (m, 1H, $HCMe_2$), 3.06 (s, 3H, $Me_{cis\,P}$), 3.60 (d, 3H, $J_{HP} = 0.9$, $Me_{trans\,P}$), 3.91 (pt, J_{HH}–$J_{HP} = 10.4$, 1H, $H_{trans\,P}$), 4.12–4.52 (m, 4H, 3 aliph, $H_{cis\,P}$), 7.03–7.09 (m, 1H, arom), 7.15–7.50 (m, 12H, arom), 8.05–8.12 (m, 1H, arom). ^{31}P{H} NMR: δ 19.90.

Minor isomer: δ 0.11 (d, 3H, $J = 6.7$, Me), 0.81–0.90 (d, 3H, Me), 2.00–2.10 (m, 1H, $HCMe_2$), 3.33 (s, 3H, $Me_{cis\,P}$), 3.60 (d, 3H, $J_{HP} = 0.9$, $Me_{trans\,P}$), 3.74 (pt, J_{HH}–$J_{HP} = 10.4$, 1H, $H_{trans\,P}$), 4.12–4.52 (m, 4H, 3 aliph, $H_{cis\,P}$), 6.94–6.99 (m, 1H, arom), 7.15–7.50 (m, 12H, arom), 8.00–8.05 (m, 1H, arom). $^{31}P\{H\}$ NMR: δ 20.88.

4.4.6. (η^2-dimethylfumarate){4-t-butyl-2-[2′-(diphenylphosphino)phenyl]-4,5-dihydroxazole]}palladium(0) (**6d**)

Yield: 48%.

^1H NMR: major isomer: δ 0.71, (s, 9H, 3 Me), 3.10 (s, 3H, $Me_{cis\,P}$), 3.60 (d, 3H, $J_{HP} = 0.8$, $Me_{trans\,P}$), 3.79 (pt, J_{HH}–$J_{HP} = 10.4$, 1H, $H_{trans\,P}$), 4.14–4.35 (m, 4H, 3 aliph, $H_{cis\,P}$), 6.96–7.01 (m, 1H, arom), 7.17–7.50 (m, 12H, arom), 8.10–8.14 (m, 1H, arom). $^{31}P\{H\}$ NMR: δ 20.95.

Minor isomer: δ 0.53, (s, 9H, 3 Me), 3.50 (s, 3H, $Me_{cis\,P}$), 3.61 (d, 3H, $J_{HP} = 0.8$, $Me_{trans\,P}$), 3.79 (pt, 1H, $H_{trans\,P}$), 4.14–4.35 (m, 3H, aliph, $H_{cis\,P}$), 4.50–4.53 (m, 1H, aliph), 6.79–6.84 (m, 1H, arom), 7.17–7.50 (m, 12H, arom), 7.16–8.20 (m, 1H, arom). $^{31}P\{H\}$ NMR: δ 21.62.

4.5. Palladium catalyzed allylic alkylation using BSA procedure

4.5.1. Palladium-catalyzed allylic alkylation of 1,3-diphenylprop-2-enyl acetate

A mixture of $[Pd(C_3H_5)Cl]_2$ (2.3 mg, 6.36 μmol) and of **2a** (7 mg, 15.9 μmol, 1.25 equiv./Pd) in CH_2Cl_2 (0.6 ml) was stirred for 15 min at r.t. To the resulting pale yellow reaction mixture a solution of rac.-1,3-diphenyl-prop-2-enyl acetate (160.1 mg, 0.68 mmol) in CH_2Cl_2 (2 ml) was added. Then dimethylmalonate (252 mg, 1.9 mmol), *N*,*O*-bis(trimethylsilylacetamide) (388 mg, 1.90 mmol) and KOAc (1.1 mg) were added. The mixture was stirred at r.t. for 22 h. Only traces of diphenylpropenyl acetate were detected by TLC (hexane–AcOEt 3:1). The solution was diluted with Et_2O and washed twice with ice cold saturated aqueous (aq.) NH_4Cl solution. The organic phase was dried (Na_2SO_4) and concentrated. CC (SiO_2, hexane–EtOAc 3:1) afforded 158 mg (76.7%) of colorless (*E*)-2-methoxycarbonyl-3,5-diphenylpent-4-enacid-methylester. ^1H NMR ($CDCl_3$): δ 3.51 (s, 3H, Me), 3.70 (s, 3H, Me), 3.95 (d, 1H, $J =$ 10.8, H-C(2)), 4.27 (dd, 1H, $J = 8.4$, 10.7, H–C(3)), 6.49 (d, 1H, $J = 15.6$, H–C(5)), 6.33 (dd, 1H, $J = 8.4$, 15.8, H–C(4)), 7.19–7.32 (m, 10H, arom). The ee value (97%) was determined on a Daicel Chiralcel OD column at $\lambda = 254$ nm, flow rate 0.3 ml min^{-1}, eluent: hexane–isopropanol 99:1.

4.5.2. Palladium-catalyzed allylic alkylation of 1-methylbut-2-enyl acetate

A mixture of $[Pd(C_3H_5)Cl]_2$ (2.32 mg, 6.36 μmol) and of **2a** (6.7 mg, 15.9 μmol) in CH_2Cl_2 (0.6 ml) was stirred for 30 min at r.t. To the resulting pale yellow mixture, a solution of rac.-1-methylbut-2-enyl acetate (84.5 mg, 0.635 mmol) in CH_2Cl_2 (3 ml) was added. Then dimethyl malonate (252 mg, 1.9 mmol), BSA (388 mg, 1.90 mmol) and KOAc (1.1 mg) were added. The mixture was stirred at r.t. for 1 h. The solution was diluted with CH_2Cl_2 (25 ml) and washed twice with ice cold sat. aq. NH_4Cl solution. The organic phase was dried (Na_2SO_4) and evaporated. CC (SiO_2, hexane–EtOAc 4:1) afforded 123 mg (93.1%) of (*E*)-2-methoxycarbonyl-3-methylhex-4-ene acid methyl ester. ^1H NMR: δ 1.06 (d, $J = 6.8$, Me), 1.63 (dd, $J = 6.4$, 1.3, Me) 2.83–2.96 (m, H–C(3)), 3.27 (d, $J = 9.1$, H–C(2)), 3.69, 3.73 (2 s, Me), 5.34 (ddq, $J =$ 15.2, 8.1, 1.3, H–C(4)), 5.51 (ddq, $J = 15.2$, 6.4, 0.8, H–C(5)). An enantiomeric excess of 18% was determined by ^1H NMR spectroscopy, using the splitting of the signal of the Me group at the stereogenic carbon center by the chiral shift reagent $Eu(hfc)_3$ ($CDCl_3$, 300 MHz, 0.5 equiv.).

4.6. Structure determinations

4.6.1. X-ray structure analysis of **3a**

Crystal data and parameters of the data collection are compiled in Table 7. Unit-cell parameters were determined by accurate centering of 25 strong reflections ($11.65 \leq \theta \leq 20.81$). Reflection intensities were collected on a four-circle diffractometer (Enraf–Nonius CAD-4), Mo Kα radiation ($\lambda = 0.71069$ Å, graphite monochromator) using ω–2θ scan. Three standard reflections were monitored every hour during data collection and showed no decrease during data collection. The usual corrections were applied. The absorption correction was determined using the ψ-scans of seven reflections [19]. The structure was solved by direct methods [20]. Anisotropic least-squares refinement against F was carried out on all non-H-atoms using the program CRYSTALS [21]. The allylic protons were refined isotropically, the positions of the remaining H-atoms were calculated. Scattering factors were taken from the International Tables of Crystallography, Vol. IV. The anion was found to be disordered. The disordered atoms were refined in two positions. Geometric restraints were applied to the disordered parts of the structure during the structure refinement.

4.6.2. X-ray structure analyses of **4a**, **5b** and **6a**

Data were collected at ambient temperature with a KappaCCD diffractometer, Mo Kα radiation ($\lambda =$ 0.71069 Å, graphite monochromator). The data were indexed and scaled by using the programs DENZO and SCALEPACK [22] and corrected for Lorenz and polariza-

Table 7
Data for the X-ray analyses

	3a	4a	5b	6a
Chemical formula	$C_{43}H_{37}F_6NOP_2Pd$	$C_{33}H_{33}F_6NOP_2Pd{\cdot}CH_2Cl_2$	$C_{29}H_{30}NO_5PPd$	$C_{33}H_{30}NO_5PPd$
Molecular weight	866.11	826.90	609.94	657.98
Crystal size (mm)	0.19 × 0.23 × 0.44	0.20 × 0.39 × 0.40	0.05 × 0.12 × 0.13	0.11 × 0.21 × 0.23
a (Å)	10.833 (3)	10.2268 (5)	9.5217 (2)	11.3108 (4)
b (Å)	11.373 (3)	10.9691 (4)	20.2317 (5)	12.2633 (4)
c (Å)	16.377 (3)	15.8743 (9)	29.1562 (6)	12.3985 (3)
α (°)	105.92 (2)	90	90	62.025 (2)
β (°)	91.07 (2)	95.611 (7)	90	76.071 (2)
γ (°)	96.91 (2)	90	90	81.362 (2)
V (Å^3)	1923.6	1772.2	5616.7	657.98
Crystal system	triclinic	monoclinic	orthorhombic	triclinic
Space group	$P\bar{1}$	$P2_1$	$Pbc2_1$	$P\bar{1}$
Z	2	2	8	2
F (000)	878	834	2488	670
ρ_{calcd} (g cm^{-3})	1.50	1.55	1.44	1.48
Absorption coefficient (mm^{-1})	0.630	0.825	0.756	0.727
θ max (°)	30.37	30.06	27.50	28.96
Number of measured reflections	12169	25196	36209	14214
Number of independent reflections	11635	9831	11749	10768
h_{min} h_{max}	$-15 \le h \le 15$	$-11 \le h \le 14$	$-12 \le h \le 12$	$-14 \le h \le 15$
k_{min} k_{max}	$-16 \le k \le 16$	$-15 \le k \le 15$	$-24 \le k \le 26$	$-16 \le k \le 16$
l_{min} l_{max}	$-15 \le l \le 16$	$-22 \le l \le 22$	$-37 \le l \le 37$	$-15 \le l \le 16$
Reflections used in reference	6559 $I \ge 3\sigma(I)$	7727 $I \ge 2\sigma(I)$	8764 $I \ge 2\sigma(I)$	7400 $I \ge 2\sigma(I)$
Number of parameters	554	515	800	378
Final R	0.047	0.045	0.042	0.049
Final R_w	0.047	0.045	0.040	0.047
Goodness-of-fit	1.051	1.013	0.989	1.047
$\Delta\rho_{max/min}$ (e Å^{-3})	−0.50/2.11	−0.78/1.05	−0.86/1.44	−0.82/1.11
Weighting scheme	Chebychev polynominal [23]			

tion effects. The structures were solved by direct methods [20]. Anisotropic least-squares refinement against F was carried out on all non-hydrogen-atoms using the program CRYSTALS [21]. The hydrogen atoms of the allylic and the alkene moieties, respectively, were located by Fourier difference synthesis and refined isotropically. All other hydrogen atoms were included in calculated positions. Scattering factors were taken from the International Tables of Crystallography, Vol. IV. The anion and the CH_2Cl_2 of **4a** were found to be disordered. One of the two crystallographically independent molecules per asymmetric unit of **5b** was partially disorderd. The disordered atoms were refined in two positions with the occupancy of 0.5 for each position. Geometric restraints were applied to the disordered parts of the structure during the structure refinement.

5. Supplementary material

Crystallographic data (excluding structure factors) for the structures reported in this paper have been deposited with the Cambridge Crystallographic Date Centre as deposition Number CCDC-179970–CCDC-179973. Copies of the data can be obtained, free of charge, on application to the CDCC, 12 Union Road, Cambridge CB2 1EZ, UK (fax: +44 (1223-336-033; e-mail: deposit@ccdc.cam.ac.uk or www; http://www.ccdc.cam.ac.uk).

Acknowledgements

The support of this project by the Swiss National Science Foundation (project Number 2000-05′8855.99.1) is gratefully acknowledged.

References

[1] (a) P. von Matt, A. Pfaltz, Angew. Chem., Int. Ed. Engl. 32 (1993) 566;
(b) J. Sprinz, G. Helmchen, Tetrahedron Lett. 34 (1993) 1769;
(c) G.J. Dawson, C.G. Frost, J.M.J. Williams, Tetrahedron Lett. 34 (1993) 3149.
[2] O. Loiseleur, M. Hayashi, N. Schmees, A. Pfaltz, Synthesis (1997) 1338.
[3] A. Lightfood, P. Schnider, A. Pfaltz, Angew. Chem., Int. Ed. Engl. 37 (1998) 2897.
[4] (a) L.M. Newman, J.M. Williams, R. McCague, G.A. Potter, Tetrahedron Asymmetry 7 (1996) 1597;

(b) T. Langer, J. Janssen, G. Helmchen, Tetrahedron Asymmetry 7 (1996) 1599.
[5] I. Sagasser, G. Helmchen, Tetrahedron Lett. 39 (1998) 261.
[6] For a review see: (a) B.M. Trost, D.L. Van Vranken, Chem. Rev. 96 (1996) 395;
(b) M.A. Lautens, A. Pfaltz, in: E.N. Jacobsen, A. Pfaltz, H. Yamamoto (Eds.), Allylic Substitution Reactions in Comprehensive Asymmetric Catalysis, vol. 2, Springer, Heidelberg, 1999, pp. 833–884.
[7] (a) A. Pfaltz, Acta Chem. Scand. 50 (1996) 189;
(b) G. Helmchen, J. Organomet. Chem. 576 (1999) 203;
(c) G. Helmchen, A. Pfaltz, Acc. Chem. Res. 33 (2000) 336.
[8] (a) J. Sprinz, M. Kiefer, G. Helmchen, M. Reggelin, G. Huttner, O. Walter, L. Zsolnai, Tetrahedron Lett. 95 (1994) 1523;
(b) N. Baltzer, L. Macko, S. Schaffner, M. Zehnder, Helv. Chim. Acta 79 (1996) 803;
(c) G. Helmchen, S. Kudis, P. Sennhenn, H. Steinhagen, Pure Appl. Chem. 69 (1997) 513;
(d) S. Schaffner, L. Macko, M. Neuburger, M. Zehnder, Helv. Chim. Acta 80 (1997) 463;
(e) S. Liu, J.F.K. Müller, M. Neuburger, S. Schaffner, M. Zehnder, J. Organomet. Chem. 549 (1997) 283;
(f) S. Schaffner, J.F.K. Müller, M. Neuburger, M. Zehnder, Helv. Chim. Acta 81 (1998) 1223;
(g) K. Selvakumar, M. Valentini, M. Wörle, P.S. Pregosin, A. Albinati, Organometallics 18 (1999) 1207;
(h) G.H. Bernardinelli, E.P. Kündig, P. Meier, A. Pfaltz, K. Radkowski, N. Zimmermann, M. Neuburger-Zehnder, Helv. Chim. Acta 84 (2001) 3233.
[9] (a) P.E. Blöchel, A. Togni, Organometallics 15 (1996) 4125;
(b) H. Hagelin, B. Åkermark, P. Norrby, Organometallics 18 (1999) 2884.
[10] (a) H. Steinhagen, M. Reggelin, G. Helmchen, Angew. Chem., Int. Ed. Engl. 36 (1997) 2108;
(b) J. Junker, B. Reif, H. Steinhagen, B. Junker, I.C. Felli, M. Reggelin, C. Griesinger, Chem. Eur. J. 6 (2000) 3281.
[11] (a) B. Jedlicka, R.E. Rülke, W. Weissensteiner, R. Fernández-Galán, F.A. Jalón, B.R. Manzano, J. Rodríguez-de la Fuente, N. Veldman, H. Kooijman, A.L. Spek, J. Organomet. Chem. 516 (1996) 97;
(b) M. Zehnder, M. Neuburger, S. Schaffner, M. Jufer, D.A. Plattner, Eur. J. Inorg. Chem. (2002) 1511.
[12] R. Fernández-Galán, F.A. Jalón, B.R. Manzano, J. Rodríguez-de la Fuente, M. Vrahami, B. Jedlicka, W. Weissensteiner, G. Jogl, Organometallics 16 (1997) 3758.
[13] U. Leutenegger, G. Umbricht, C. Fahrni, P. von. Matt, A. Pfaltz, Tetrahedron 48 (1992) 2143.
[14] P. Barbaro, P.S. Pregosin, R. Salzmann, A. Albinati, R.W. Kunz, Organometallics 14 (1995) 5160.
[15] T. Ukai, H. Kawazura, Y. Ishii, J.J. Bonnet, J.A. Ibers, J. Organomet. Chem. 65 (1974) 253.
[16] D. Obrecht, U. Bohdal, R. Ruffieux, K. Müller, Helv. Chim. Acta 77 (1994) 1423.
[17] D. Obrecht, U. Bohdal, C. Broger, D. Bur, C. Lehmann, R. Ruffieux, P. Schönholzer, C. Spiegler, K. Müller, Helv. Chim. Acta 78 (1995) 563.
[18] G. Koch, G.C. Lloyd-Jones, O. Loiseleur, A. Pfaltz, R. Prétôt, S. Schaffner, P. Schnider, P. von Matt, Recl. Trav. Chim. Pays-Bas. 114 (1995) 206.
[19] A.C.T. North, D.C. Phillips, F.S. Mathews, Acta Crystallogr. 24 (1968) 351.
[20] A. Altomare, M.C. Burla, M. Camalli, G. Cascarano, C. Giaccovazzo, A. Gualgliardi, G. Polidori, J. Appl. Crystallogr. 27 (1994) 435.
[21] D. Watkin, Crystals (issue 9), Chemical Crystallography Laboratory, Oxford, 1990.
[22] J.R. Carruthers, D.J. Watkin, Acta Crystallogr., A 35 (1979) 698.
[23] Z. Otwinowsky, W. Minor, Processing of X-ray diffraction data in oscillation mode in methods in enzymology, in: C.W. Carter, R.M. Sweet (Eds.), Macromolecular Crystallography, vol. 276 (Part A), Academic Press, London, 1997, pp. 307–326.